One simulation, different conclusions—the baseline period makes the difference!

Environmental Research Letters

One simulation, different conclusions–the baseline period makes the difference!

S Liersch[1], M Drews[2], T Pilz[1], S Salack[3], D Sietz[1], V Aich[1,4], M A D Larsen[2], A Gädeke[1], K Halsnæ s[2], W Thiery[5], S Huang[6], A Lobanova[1], H Koch[1] and F F Hattermann[1]

[1] Potsdam Institute for Climate Impact Research (PIK), Member of the Leibniz Association, P.O. Box 60 12 03, D-14412 Potsdam, Germany
[2] Technical University of Denmark (DTU), Produktionstorvet, 2800 Kongens Lyngby, Denmark
[3] WASCAL Competence Center, Blvd Moammar El-Khadafi, 06BP 9507, Ouagadougou 06, Ouagadougou, Burkina Faso
[4] Global Climate Observing System (GCOS) Secretariat, c/o World Meteorological Organization (WMO)
[5] Vrije Universiteit Brussel (VUB), Department of Hydrology and Hydraulic Engineering, Brussels, Belgium
[6] The Norwegian Water Resources and Energy Directorate (NVE), PO Box5091, Majorstua, 0301 Oslo, Norway

E-mail: liersch@pik-potsdam.de

OPEN ACCESS

RECEIVED
20 May 2020

REVISED
23 June 2020

ACCEPTED FOR PUBLICATION
8 July 2020

PUBLISHED
18 September 2020

Keywords: baseline period, climate impacts, climate projections, flexible baseline

Abstract

The choice of the baseline period, intentionally chosen or not, as a reference for assessing future changes of any projected variable can play an important role for the resulting statement. In regional climate impact studies, well-established or arbitrarily chosen baselines are often used without being questioned. Here we investigated the effects of different baseline periods on the interpretation of discharge simulations from eight river basins in the period 1960–2099. The simulations were forced by four bias-adjusted and downscaled Global Climate Modelsunder two radiative forcing scenarios (RCP 2.6 and RCP 8.5). To systematically evaluate how far the choice of different baselines impacts the simulation results, we developed a similarity index that compares two time series of projected changes. The results show that 25% of the analyzed simulations are sensitive to the choice of the baseline period under RCP 2.6 and 32% under RCP 8.5. In extreme cases, change signals of two time series show opposite trends. This has serious consequences for key messages drawn from a basin-scale climate impact study. To address this problem, an algorithm was developed to identify flexible baseline periods for each simulation individually, which better represent the statistical properties of a given historical period.

1. Introduction

In the context of climate change mitigation and adaptation, decision-makers generally call for information about impacts of projected changes in a specific region at different global warming levels or in certain future periods. They need answers to questions like: 'Can we expect an increase or decrease in water availability, extreme events, such as floods, droughts, storm surges or heatwaves, around the year 2030, 2050 or by the end of the 21st century? And what will be the consequences for, e.g. crop production, renewable electricity generation?' To answer such questions, regional climate impact modelers face a variety of challenges, which relate to technical, methodological, and communication issues of simulation results [1] and corresponding recommendations under uncertainties in a comprehensible way.

Adding to technical and methodological challenges includes, e.g. the choice of climate scenarios, climate and impact models, the use of bias-adjustment methods, and model calibration and validation periods. The performance of a climate model is usually measured against its ability to represent spatial patterns and trends in the historical climate. Sometimes the performance is used to assign weights to individual models within a model ensemble [2–7]. The uncertainty cascade in the impact modeling is basically associated with model structure, model parameterization, and input data quality [8–15].

After the simulations have been carried out, the question about the baseline period used to compare future simulation results to, will arise. Where future scenario periods are usually defined to reflect the decision maker's planning horizon, baseline periods are often chosen arbitrarily or are based on existing

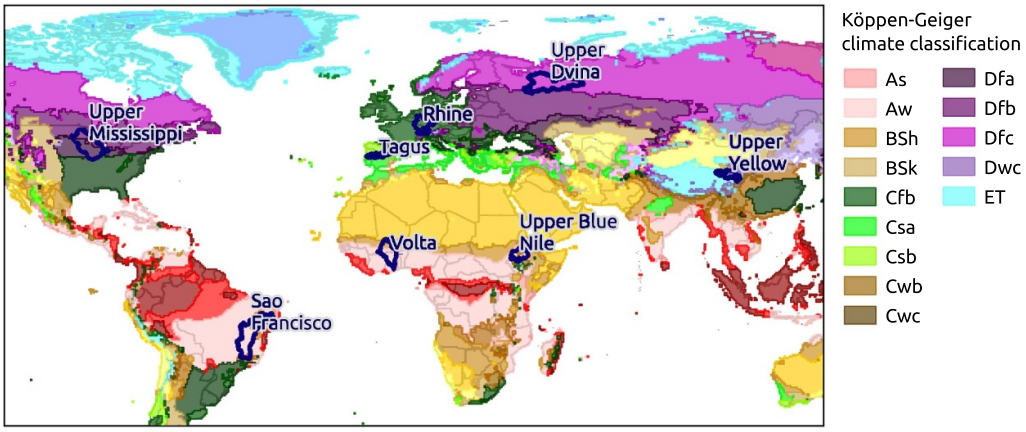

Figure 1. Map of case study river basins and climate zones. Source climate zones: Kottek *et al* (2016) [30].

standards. However, choosing a baseline period is a sensitive issue and can be easily instrumentalized to support specific conclusions, whether intentionally or not.

The World Meteorological Organization (WMO) recommends to use the 30-year period of 1961–1990 as the climate normal when comparing with future periods and that this should be maintained as a reference for monitoring long-term climate variability and change [16, 17]. Beyond that, a regularly updated 30-year baseline period, currently 1981–2010, should be employed to give people a more recent context for understanding weather and climate extremes and forecasts [17–19]. The Intergovernmental Panel on Climate Change (IPCC) used the 20-year period 1986–2005 as the baseline in many graphs in the Fifth Assessment Report [20] and will use the years 1995–2014 in its Sixth Assessment Report. So, what are climate impact modelers supposed to do? Which baseline should they select and does it actually matter?

At the global or continental scale, it is virtually impossible to choose a baseline period whose climate is represented realistically by all climate models. An arbitrary determination of global baselines is therefore justifiable. However, global and regional climate simulations are often not designed to synchronize with real year to year patterns and events [21], which creates a communication challenge, particularly in regional impact studies. For example, some climate models depict the mid-1980s as a period with above-normal rainfall, when in reality a drought hit West Africa. Others simulate the extraordinary wet 1950s and 1960s as very dry. Nevertheless, well-established global baseline periods are often used unquestioningly in regional impact studies, although the real-life statistical properties of the specific historical period may not be adequately represented by climate model simulations, therefore, also not in subsequent applications.

Even though the implications of the choice of baseline periods for the interpretation of simulation results are well known, little attention has been paid to them in the climate impact community. Ruokolainen and Räisänen (2007) [22] analyze the sensitivity of forecasts to the choice of different baselines in Southern Finland. Razavi *et al* (2015) [23] emphasize that different length of baseline periods may lead to different conclusions about stationarity/non-stationarity. Hawkins and Sutton (2016) [18] discuss the choice of climate reference periods when comparing global air temperature projected by climate models with observations. Huang *et al* (2018) [24] depict future flood characteristics in future periods in four river basins based on different 30-year baseline periods. Snell *et al* (2018) [25] highlight the sensitivity to the choice of baseline climate in dynamic forest modeling in the Alps. Baker *et al* (2016) [26] assessed the impact of six different climate baselines on projections of African bird species' responses to future climate change. Although this issue has been addressed as a side effect in several other studies, it has generally not been considered important to form the focal point for systematic research.

The present study systematically investigates the effect of the choice of the baseline period on the interpretation of simulation results. It provides examples from eight river basins located in various climate zones, where changes in projected future discharge are estimated based on WMO and IPCC baselines using four bias-adjusted and downscaled Global Climate Models (GCMs) from the Inter-Sectoral Impact Model Intercomparison Project (ISIMIP) [27–29]. An index measuring the similarity between two time series is introduced and was used to assess the sensitivity of choosing different baseline periods. We developed an algorithm to overcome the problem in cases of substantial deviations. It identifies a baseline period, which consists of similar basic statistical properties as the historical period and is flexible in terms

of length and timing. Although the main focus of this study is the analysis of river discharge, the method is in principle applicable to any time series variable, such as meteorological data, crop yields, emissions of greenhouse gases, hydropower potentials and so on.

2. Materials and methods

2.1. Study sites

The impact of different baseline periods was investigated by using simulated river discharge from eight exemplary river basins located in various climate zones from equatorial to polar (figure 1 and table 1). The simulations were carried out within the framework of various research projects (see references in table 1). What they have in common is the hydrological model, the same four forcing GCMs, and the simulation period they cover (1960–2099), which guarantees consistency across the study basins.

2.2. Data

The investigation was conducted using annual mean discharge *MQ*, derived from simulated daily discharge from eight river basins, based on climate model input from four GCMs in the period 1960–2099. The discharge was simulated with the semi-distributed, eco-hydrological soil and water integrated model (SWIM) [35, 36]. The downscaled and bias-adjusted GCM climate simulation data were provided by ISIMIP [27–29, 37] for the GFDL-ESM2M, HadGEM2-ES, IPSL-CMA5-LR, and MIROC5 models. The aim is to provide harmonized climate simulation input to impact modelers and thereby to support the intercomparison of global and regional impact studies.

2.3. Baseline periods

The impact of the baseline period on the interpretation of changes in simulated future river discharge was investigated by using two baselines established by the WMO [17] and the IPCC [20]. The *WMO baseline* covers the 30 years 1961–1990 and the *IPCC baseline* the 20 years 1986–2005. Other IPCC reports use also different and longer baseline periods. However, we chose the above-mentioned baseline here, as it is used in many graphs in the IPCC AR5 report [20] and is therefore likely to tempt impact modelers to use it as a standard in their studies. Interestingly, the central limit theorem dictates that at least 30 samples are needed if we assume a normal distribution and to ample natural variability [38] as in the case of the WMO [16, 19]. From this perspective, the *IPCC baseline* is thereby too short, especially if variables with a high degree of natural variability are considered, e.g. river discharge. However, one could argue that the sample size is sufficiently large, if the combination of years in the baseline period times the number of models exceeds a critical threshold, which is given in the case of the IPCC (20 years times 40^+ GCMs). In addition, the selection of the baseline period should strike the balance between being statistically robust and representative of the target conditions (e.g. 'present-day climate'). For rapidly changing variables, such as for instance extreme temperatures, reference periods of 30 years or longer might be considered insufficiently representative of the target conditions.

In this study, we hypothesize that the baseline period is a subset that accurately represents some basic statistical properties of a historical period, here defined as 1960–2005. An algorithm was developed to identify for each simulation a baseline period of variable length within a given historical period. The algorithm searches for a baseline period whose mean, minimum, and maximum values correspond to those of the historical period. In line with common practice of hydro-climatic impact studies, the baseline period should cover at least 30 years. The statistical properties of the baseline period are allowed to deviate from those of the historical period by not more than a user-defined threshold, e.g. 5%. If the algorithm is not able to find an appropriate baseline with $n = 30$ years, n is incremented by 1. The resulting baseline period is therefore flexible in terms of its length and starting year and is called hereafter 'flexible baseline'. The corresponding function, implemented in R, is provided in appendix A. It works only for annual series but can be easily adapted for monthly or daily series.

To account for the possibility of a linear climate change trend in the historical discharge, the algorithm was tested using a time series detrended using the first (linear) differencing method (appendix B). In general, the differences in the results were found to be minor and the identified baseline periods to be longer. To avoid accidentally removing or suppressing some of the extreme years by applying a linear operation, results shown below are all based on the original data.

2.4. Similarity index

The *MQ* time series was used to compute the relative change between a specific baseline and a corresponding future period as follows:

$$\Delta MQ_{i,j} = \frac{\overline{MQ}_{future,i} - \overline{MQ}_{base,j}}{\overline{MQ}_{base,j}}, \qquad (1)$$

where $\overline{MQ}_{base}$ is the average of the annual values of a specific baseline period and $\overline{MQ}_{future}$ the average of a future period. The index i refers to different future periods with central years between 2020 and 2080, i.e. 61 time steps. The index j represents the different baselines (WMO, IPCC, and flexible baseline), where the length of the baseline determines the number of years around the central years in corresponding $\overline{MQ}_{future}$ periods.

The mean absolute deviation between two ΔMQ time series, e.g. $\Delta MQ_{WMO,i}$ for the WMO and

Table 1. River basins.

River basin	Gauge	Area [km^2]	Region	Climate zone
Northern Dvina (DVI) [31]	Ust-Pinega	348.000	Europe, Russian Federation	Snow (Dfc)
Rhine (RHI) [24]	Lobith	160.000	Europe	Warm temperate (Cfb)
São Francisco (SFC) [32]	Outlet	640.000	S America	Equatorial (Aw, As), arid (BSh)
Tagus (TAG) [31]	Almourol	70.000	S Europe	Warm temperate (Csa, Csb)
Upper Blue Nile (UBN) [4, 33, 34]	El Diem	175.000	E Africa	Arid (Aw), warm temperate (Cwb)
Upper Mississippi (UMI) [24]	Alton	440.000	N America	Snow (Dfa, Dfb)
Volta (VOL)	Outlet	403.000	W Africa	Equatorial (Aw), arid (BSh)
Upper Yellow (YEL) [24]	Tangnaihai	121.000	China	Polar (ET), snow (Dwc)

$\Delta MQ_{IPCC,i}$ for the IPCC baseline, over all $k = 61$ time steps was then quantified as:

$$D = \frac{1}{k}\sum_{i=1}^{k} \mid \Delta MQ_{WMO,i} - \Delta MQ_{IPCC,i} \mid . \quad (2)$$

The deviation was then re-scaled by a user-defined deviation threshold $D_{\max}$ to an agreement score value

$$AS = \begin{cases} 1 - \frac{D}{D_{\max}} & \text{if} \quad D \leq D_{\max} \\ 0 & \text{if} \quad D > D_{\max} \end{cases} \quad (3)$$

This *Agreement Score* ranges between one (no deviation, perfect agreement) and zero (deviation larger than the threshold). In this study a threshold value of $D_{\max} = 25\%$ was defined, because deviations in discharge projections > 25% that are solely based on different baselines, were considered to be very large and indicative for a substantial difference. For other applications (e.g. greenhouse gas emissions, temperature, precipitation, wind speed) or by using not relative but absolute changes for $\Delta MQ_{i,j}$, other threshold values might be more appropriate.

Apart from the deviation based on the choice of different baselines, we quantified the direction of change signals *CS* as

$$CS_{i,j} = \begin{cases} 1 & \text{if } \Delta MQ_{i,j} > 0.01 \\ 0 & \text{if } -0.01 \leq \Delta MQ_{i,j} \leq 0.01, \\ -1 & \text{if } \Delta MQ_{i,j} < -0.01 \end{cases} \quad (4)$$

compared the agreement between two baselines for the future periods by setting

$$AC_i = \begin{cases} 1 & \text{if } CS_{WMO,i} = CS_{IPCC,i} \\ 0 & \text{if } CS_{WMO,i} \neq CS_{IPCC,i} \end{cases} \quad (5)$$

to eventually derive the average agreement in the direction of the change signal by

$$AC = \frac{1}{k}\sum_{i=1}^{k} AC_i. \quad (6)$$

Finally, a *Similarity Index* was defined as

$$SI = \frac{AS + AC}{2}. \quad (7)$$

A value of zero is derived if the selection of a baseline has a large impact on the interpretation of results of an impact study while the optimum value of $SI = 1$ is achieved if the choice of the baseline would have no influence at all. An intermediate value of $SI = 0.5$ can be derived if the absolute deviations are large with respect to the user-defined $D_{\max}$ value, but both baselines show the same directions of change over all possible future periods. Likewise, a value of approximately 0.5 is obtained when the choice of different baselines results in a bias with small absolute deviation with respect to $D_{\max}$, although the directions of change deviate for all possible future periods.

The computation of *SI* was also tested by integrating other factors, such as agreement in standard deviation or R^2, but the results achieved with a more complex indicator were not considered to be more meaningful than those achieved with the simplistic approach. The *SI* was also used to assess the sensitivity of the choice of the baseline depending on the GCM and the climate zone.

3. Results and discussion

This section shows to what extent the choice of the baseline alone can influence the interpretation of simulation results.

Figure 2 shows future ΔMQ series for selected river basins relative to *MQs* in the WMO and IPCC baselines. Future change signals and magnitudes of change can be extremely different between the two ΔMQ series (figures 2(a) and (c)). Both examples are therefore characterized by low *SI* values of 0.24 and 0.19, respectively, which indicate large differences of *MQ* values in the respective baselines. They also demonstrate that neither the results based on the one nor the other baseline generally tends to suggest higher or lower future ΔMQ, a phenomenon

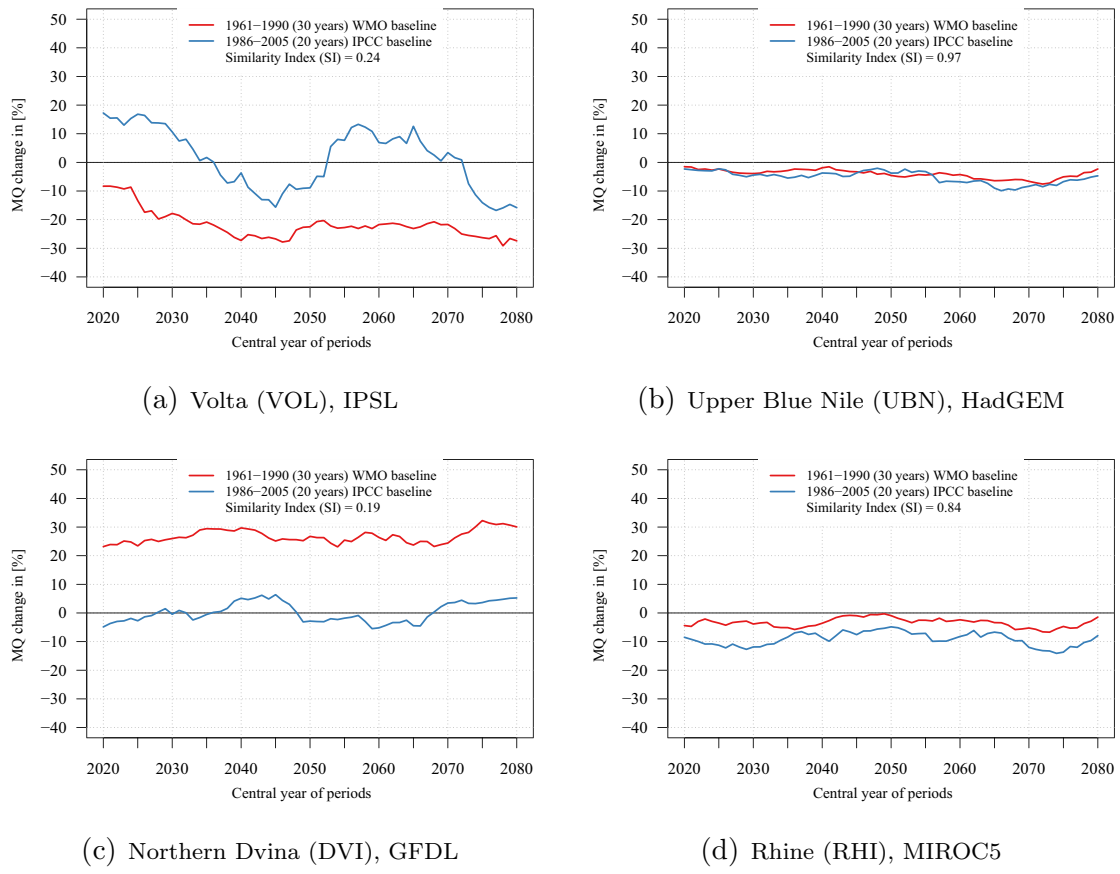

Figure 2. Relative change in *MQ* of central years in four river basins using four different GCMs under RCP 2.6. Changes are relative to *MQ* in WMO and IPCC baselines.

Table 2. Similarity index *SI* between WMO and IPCC ΔMQ series (mean of period 2020–2080), RCP 2.6.

	DVI	RHI	SFC	TAG	UBN	UMI	VOL	YEL	Average
GFDL	0.19	0.82	0.82	0.68	0.93	0.49	0.54	0.44	0.61
HadGEM	0.93	0.53	0.62	0.65	0.97	0.35	0.75	0.62	0.68
IPSL	0.43	0.65	0.15	0.55	0.88	0.73	0.24	0.95	0.57
MIROC5	0.86	0.84	0.81	–	0.19	0.92	0.8	0.62	0.72
Average	0.60	0.71	0.60	0.62	0.74	0.62	0.58	0.66	

also found in river basins shown in appendix C. Considering the example of the Northern Dvina River basin (figure 2(c)), one would conclude that future ΔMQ does not change substantially but rather fluctuates around the historical mean if the IPCC baseline is used. A completely different conclusion would be drawn with the WMO baseline, where ΔMQ is projected to increase between 22 and 32%. This illustrates how the choice of the baseline period, based on the same model simulation, would lead to conflicting recommendations for adaptation strategies.

Figures 2(b) and (d) show examples of future ΔMQ where it apparently does not matter which baseline is used as reference. The corresponding *SI* values of 0.97 and 0.84 are therefore much higher than in the other two examples. Recommendations for adaptation strategies would consequently be much less dependent on the choice of the baseline period in these cases.

A visual assessment of the ΔMQ series with the corresponding *SI* values in figure 2 is conclusive, where low *SI* values indicate a high sensitivity to the choice of the baseline period and high *SI* values a low sensitivity. As with model performance indicators (e.g. R^2, PBIAS), an evaluation of which value ranges indicate actually a good or poor fit, or in the case of the *SI*, which values represent high or low sensitivity, remains somehow subjective. In the context of simulated river discharge, we propose *SI* values below 0.5 to indicate high sensitivity.

The choice of the baseline period has the highest impact on the interpretation of simulation results performed with the IPSL model and the lowest impact with the MIROC5 model. However, the average GCM *SI* value (table 2) does not imply that this assumption is true for all basins and all RCPs. The results for RCP 8.5 are slightly different, where the highest *SI*

Table 3. Ensemble mean ΔMQ in selected future periods in [%] relative to MQ of WMO, IPCC, and flexible baseline, RCP 2.6.

	2040			2060			2080		
Basins	WMO	IPCC	Flex.	WMO	IPCC	Flex.	WMO	IPCC	Flex.
DVI	9.2	−4.7	7.9	7.2	−4.7	6.0	8.0	0.7	6.6
RHI	−4.2	−5.4	−4.8	−0.8	−3.1	−1.4	3.0	2.1	2.3
SFC	−12.8	−6.3	−12.1	−14.0	−8.0	−10.4	−5.0	8.8	−4.5
TAG	−5.6	−3.7	−5.6	0.3	0.0	−0.3	7.6	11.5	7.0
UBN	18.5	14.7	16.0	22.4	15.7	19.8	17.9	13.3	15.2
UMI	−8.5	−7.9	−8.4	−4.1	−0.7	−3.5	1.1	3.9	2.2
VOL	10.6	8.8	11.2	9.3	16.6	10.1	2.4	7.3	3.3
YEL	1.8	5.5	4.0	7.7	13.3	9.7	5.6	11.8	7.7
Mean diff.	4.2			5.5			5.5		
Min. diff.	0.6			0.3			0.8		
Max. diff.	13.9			11.9			13.9		
Median diff.	2.8			5.8			4.7		

Last four rows indicate differences between WMO and IPCC ΔMQ series
Flex. = flexible baseline

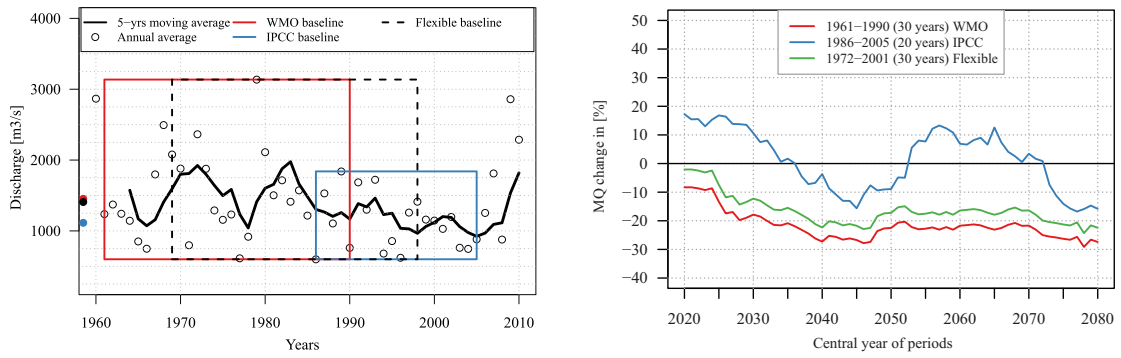

(a) Baseline periods (b) Discharge change

Figure 3. (a) MQ in the Volta River basin simulated with IPSL and the range and timing of baselines, (b) relative change in MQ of central years in the Volta basin with IPSL under RCP 2.6 (WMO, IPCC, and flexible baselines).

value is also achieved with the MIROC5 model, but the lowest values with GFDL (table D1).

Assuming an SI threshold of 0.5, it mattered in 25% of the simulations under RCP 2.6 (table 2) and in 32% under RCP 8.5 (table D1), whether the one or the other baseline was used to assess future changes. There are basically two options to deal with simulations resulting in $SI \leq 0.5$: (i) discuss the uncertainties and/or (ii) choose a different baseline that represents the basic statistical properties of the historical period more consistently, e.g. by using the proposed algorithm in appendix A.

To exemplify, the projected discharge changes with an additional flexible baseline for the Volta River basin is shown in figure 3. It explains why the results derived with both baselines are so different. The MQ values for the WMO and IPCC baselines are 1454 and 1115 m^3s^{-1}, respectively. The algorithm identifies the 30-year flexible baseline 1972–2001 with an MQ value of 1361 m^3s^{-1}, which is much closer to the MQ of the WMO than to the MQ of the IPCC baseline. Furthermore, the range of values of the IPCC baseline is much smaller. Where the years with the lowest discharges are identical, the highest MQ is only 1800 but 3150 m^3s^{-1} in the WMO and flexible baselines. This would make a significant difference in an analysis of the distribution of wet, dry, and extreme years.

Results from all river basins under both RCPs show that the projected ΔMQ series using flexible baselines lie either in between or outside WMO and IPCC ΔMQ. But, in all cases, they resemble the WMO more than the IPCC ΔMQ series (figures in appendix C), which is an indication that also the length of the baseline period matters.

Table 3 shows relative differences of ensemble ΔMQ between WMO, IPCC, and flexible baselines for all river basins around the central years 2040, 2060, and 2080 for RCP 2.6 and table E2 for RCP 8.5. In the Northern Dvina River basin (DVI) in 2040 and 2060 and in the São Francisco River basin (SFC) in 2080, the ensemble mean projects opposing change signals between WMO and IPCC baselines, with absolute differences up to 13.9% under RCP 2.6 and almost 20% under RCP 8.5. Relative differences between WMO and IPCC baselines are lower if the ensemble mean is considered (appendix E), but can be very high for individual models, as was shown in

figures 2(a) and (c). As with individual models, the ensemble mean ΔMQ series of the flexible baseline are always more similar to the WMO than to the IPCC ΔMQ series.

The sensitivity ($SI \leq 0.5$) of the choice of the baseline period for different climate zones is inconclusive (table 2 and table E2). A larger sample size of catchments from various climate zones is required to make more robust statements. However, the lowest sensitivity was achieved in warm temperate climates (C) represented by the Rhine, Tagus, and Upper Blue Nile River basins.

4. Conclusions

This study demonstrates how solely the choice of a baseline period can influence the interpretation of discharge projections in eight river basins using climate input from four bias-adjusted GCMs. To evaluate whether the choice of either the well established 30 years (1961–1990) WMO [17] or the more recent 20 years (1986–2005) IPCC [20] baseline matters, a similarity index *SI* was introduced as a measure to compare the two resulting time series of future change. In about 25% of the simulations under RCP 2.6 and in 32% under RCP 8.5, large quantitative differences and/or opposite signals of change were found, with at least one case of major discrepancies in each river basin. The deviations for selected future periods can be so large that they range from −5% to +45% for a given central year. These figures indicate that different recommendations for action could possibly be derived in at least every fourth case.

No systematic differences in the direction of change using either baseline period could be identified. Neither the results based on the WMO nor those based on the IPCC baseline tend to generally project higher or lower future river discharge.

4.1. Choosing baseline periods

Given that a baseline period is normally a subset of the historical period, it should represent its basic statistical properties. From a formal statistical perspective, a minimum length of 30 years is highly recommended for regional impact studies, particularly when using integrated variables, such as river discharge. We developed an algorithm, which identifies for each simulation a flexible baseline of variable length and variable start year representing the basic statistical properties of a given historical period. In about 20% of the 32 simulations, the flexible baselines were longer than 30 years, highlighting the importance of longer-term perspectives to more confidently quantify historic reference variability when developing adaptation strategies. The use of flexible baselines helps to reduce uncertainty in the interpretation of model simulations in cases where standard baseline periods do not capture the variability of the historical period. If multiple ranges of uncertainty, such as those implied by the impact modeling cascade and multi-criteria baseline selection, are combined, the central limit theorem implies that central tendencies are favored at the expense of extremes [39].

4.2. Regional context

At the local and regional scales, it is important to take region-specific characteristics into account, where other factors that are largely independent of past climate variability may also influence the choice of a representative baseline period, e.g. degree of human impact (land use/cover change, reservoirs, irrigation). In this context, it is reasonable to question whether the baseline period should represent rather natural conditions (far back in time with low human impact) or more recent conditions (with strong human impact). Another reason why the application of standard baseline periods is questionable is that they are often detached from reality. If a baseline period is chosen that, for example, was characterized by severe droughts in reality and future simulations project relatively drier conditions (even though the simulated baseline was above normal), stakeholders may interpret that the future will be drier than the driest period they have experienced in their lives. Using flexible baselines is a solution to better tailor information to the needs of decision makers while addressing the challenge of uncertainty transparently and efficiently.

4.3. Ensemble mean versus single model simulations

Generally, the interpretation of results based on model ensembles is less sensitive to the choice of baseline periods than for single model simulations. Nevertheless, in three cases, even the ensemble mean using the WMO and IPCC baselines projected opposite change signals in selected future periods.

4.4. Outlook

An analysis of results based on monthly or daily time series or a focus on extremes rather than the average might reveal an even higher sensitivity to chosen baseline periods than the annual time series used in this study. An improvement of the algorithm to identify flexible baseline periods, in terms of incorporating more sophisticated statistical parameters and tests, might be necessary if applied to monthly or daily time series.

4. Acknowledgment

This research was funded in the frame of the CIREG project (https://cireg.pik-potsdam.de/en/) by ERA-NET Co-fund action initiated by JPI Climate, funded by BMBF (DE), FORMAS (SE), BELSPO (BE), and IFD (DK) with co-funding by the European Union's Horizon 2020 Framework Program (Grant 690462).

We thank our colleagues Dr Valentina Krysanova, Iulii Didovets, Samuel Fournet, and the two anonymous reviewers for their inspiring ideas.

Appendix A. Baseline algorithm (R)

```
#-------------------------------------------------------------
assess_deviations <- function(ts, ncycle, base_length,
 ts.stats) {
    # numeric vectors storing deviations between
    # mean maximumm, and minimum values
    # between flexible baseline and entire historical period
    dev.mean <- numeric(ncycle)
    dev.max <- numeric(ncycle)
    dev.min <- numeric(ncycle)
    for ( y in 1:ncycle ) {
        sel <- ts[y:(y + base_length - 1)]
        dev.mean[y] <- (mean(sel, na.rm = T) -
                            as.numeric(ts.stats[1])) / as.
numeric(ts.stats[1]) * 100
        dev.max[y] <- (max(sel, na.rm = T) -
                           as.numeric
(ts.stats[2])) / as.numeric(ts.stats[2]) * 100
        dev.min[y] <- (min(sel, na.rm = T) -
                           as.numeric
(ts.stats[3])) / as.numeric(ts.stats[3]) * 100
    }
    assess_deviations <- list(dev.mean, dev.max, dev.min)
}
#-------------------------------------------------------------
#-------------------------------------------------------------
select_baseline <- function(ts, first_year, last_year, base_
length, thresh.dev) {
    # This function returns a logical vector,
    # where TRUE-values indicate the years of the "best"
 baseline period.
    # The "best" baseline period is defined as
    # the period of a given length (base_length)
    # with the lowest deviations between mean, max, and
 min values
    # between the flexible baseline period and the entire
 historical period.
    # INCOMING VARIABLES
    # ts = time series of (annual) values
    # first_year = first year of time series
    # last_year = last year of time series
    # base_length = minimum number of years in baseline
 periods
    # number of cycles from first to last year, depending on
 base_length
    ncycle <- last_year - first_year + 2 - base_length
    nyears <- last_year - first_year + 1
    # statistics of entire time series
    ts.mean <- mean(ts, na.rm = T)
    ts.max <- max(ts, na.rm = T)
    ts.min <- min(ts, na.rm = T)
    ts.stats <- list(ts.mean, ts.max, ts.min)
    #-------------------------------------------------------------
    # iterations
    #-------------------------------------------------------------
    bs_length <- base_length - 1
    nc <- ncycle
    index <- NULL
    ids.valid <- NULL
    select_baseline <- vector(mode = "logical", length =
nyears)
    while ( length(ids.valid) == 0 ) {
        # add 1 year to baseline period if necessary during
iterations
        bs_length <- bs_length + 1
        # if length of baseline period equals entire period:
        # - return entire period and exit function
        if ( bs_length == nyears ) {
            print( "length of baseline period equals entire
period" )
            select_baseline[1:length(select_baseline)] <- T
            return(select_baseline)
        }
        # compute the number of cycles possible to iterate
the baseline
        # period through the entire period
        nc          <- last_year - first_year + 2 - bs_length
    # compute mean, max., and min. deviations between
    # baseline and entire period
        dev.stats <- assess_deviations(ts, nc, bs_length, ts.stats)
        # evaluate results against given threshold
        ids.valid <- which(abs(unlist(dev.stats[1])) < thresh.
dev &
                    abs(unlist(dev.stats[2])) < thresh.dev &
                    abs(unlist(dev.stats[3])) < thresh.dev)
        if ( length(ids.valid) >= 1 ) {
            if ( length(ids.valid) == 1 ) {index <- ids.valid }
            if ( length(ids.valid) > 1 ) {
                # find tuple with lowest sum
                sum.tuple<- abs(unlist(dev.stats[1]))
[ids.valid] +
                            abs(unlist(dev.stats[2]))[ids.valid] +
                            abs(unlist(dev.stats[3]))[ids.valid]
                index          <- ids.valid[which(sum.tuple =
= min(sum.tuple))]
            }
        }
    }
    select_baseline[index:(index + bs_length - 1)] <- T
    return(select_baseline)
}
#-------------------------------------------------------------
```

Appendix B. Using detrended historical data

Figure B1. Length and timing of baseline periods 'original' and detrended.

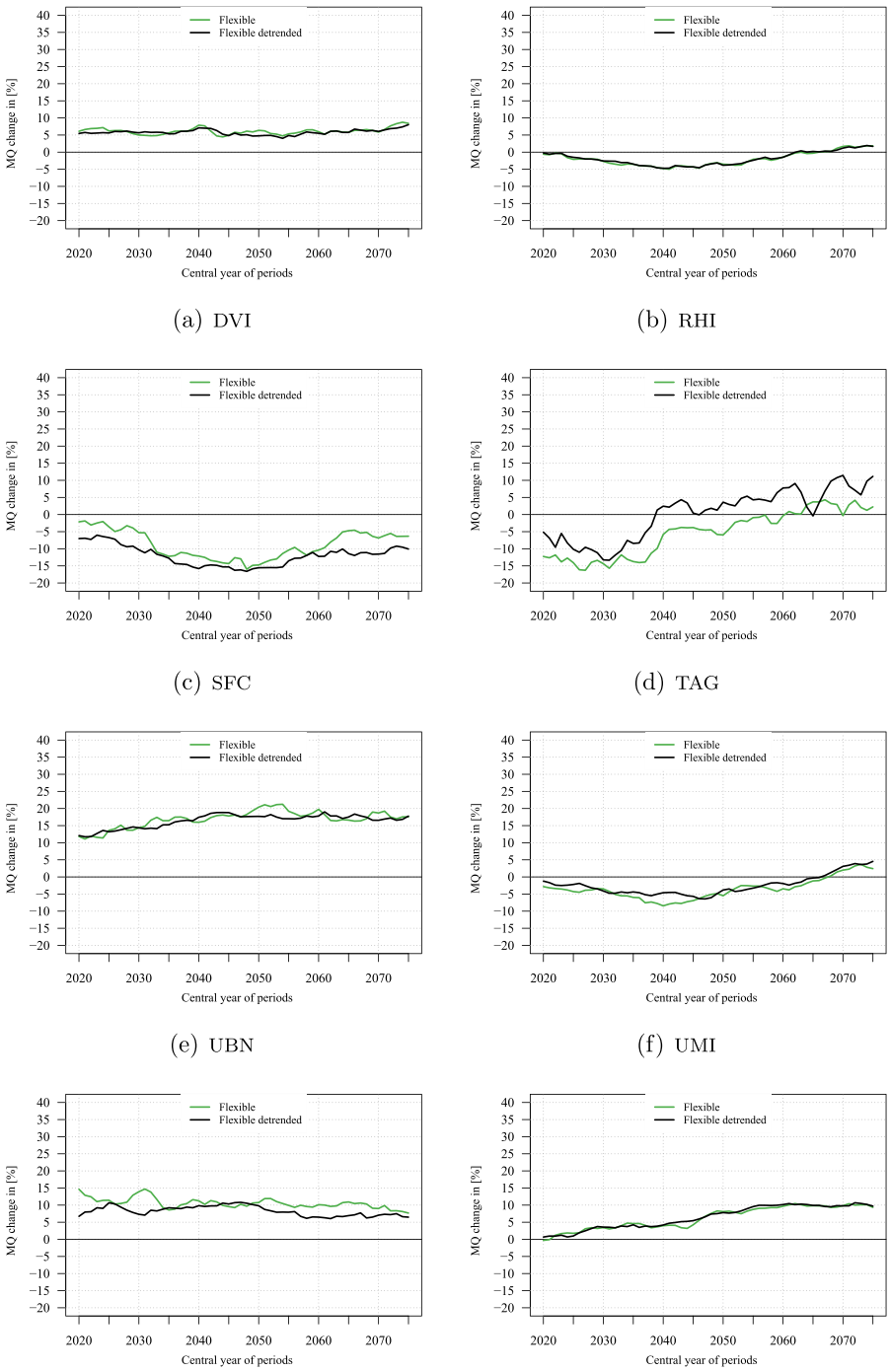

Figure B2. Ensemble mean MQ changes using the 'original' flexible baseline and the detrended baseline.

Appendix C. Relative discharge changes

C.1. RCP 2.6

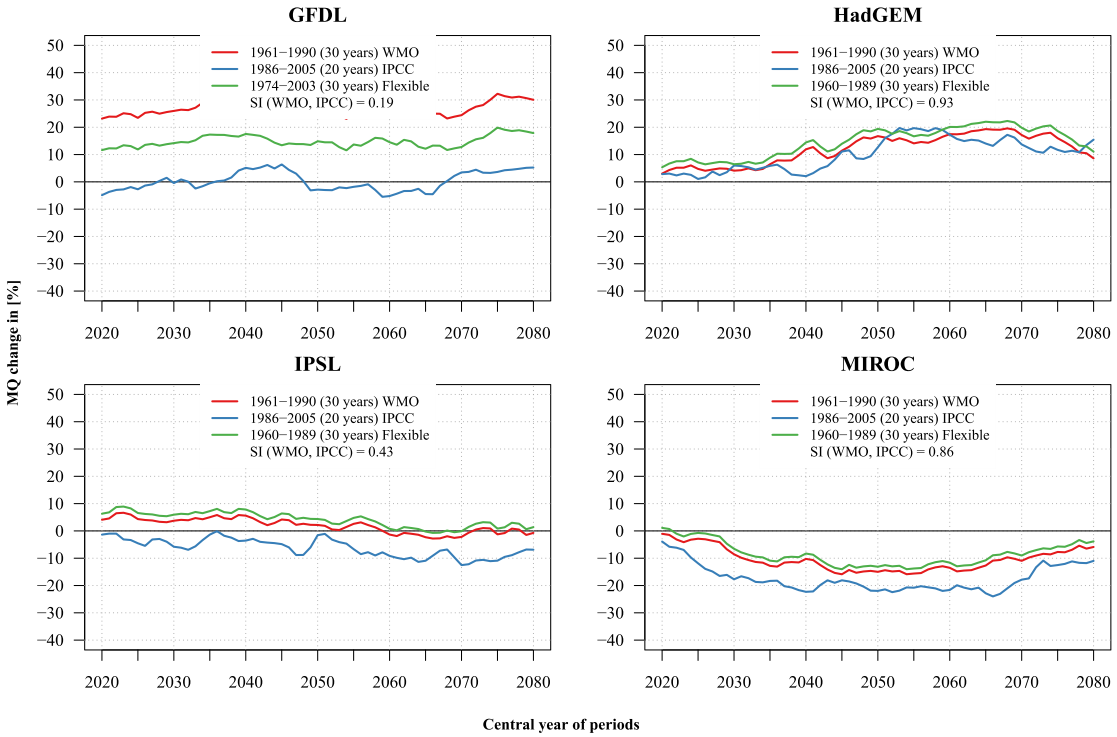

Figure C3. Relative change in mean discharge of central years. Northern Dvina River basin (DVI) under RCP 2.6. Changes are relative to mean annual discharge in WMO and IPCC baseline periods.

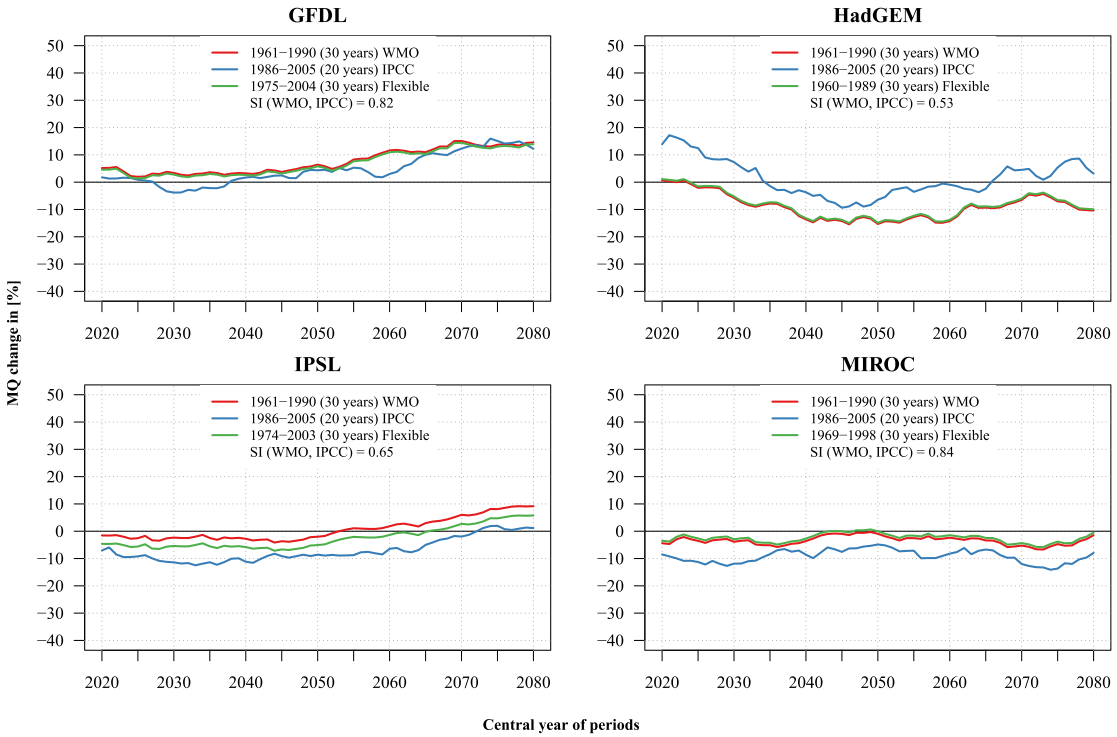

Figure C4. Relative change in mean discharge of central years. Rhine River basin (RHI) under RCP 2.6. Changes are relative to mean annual discharge in WMO and IPCC baseline periods.

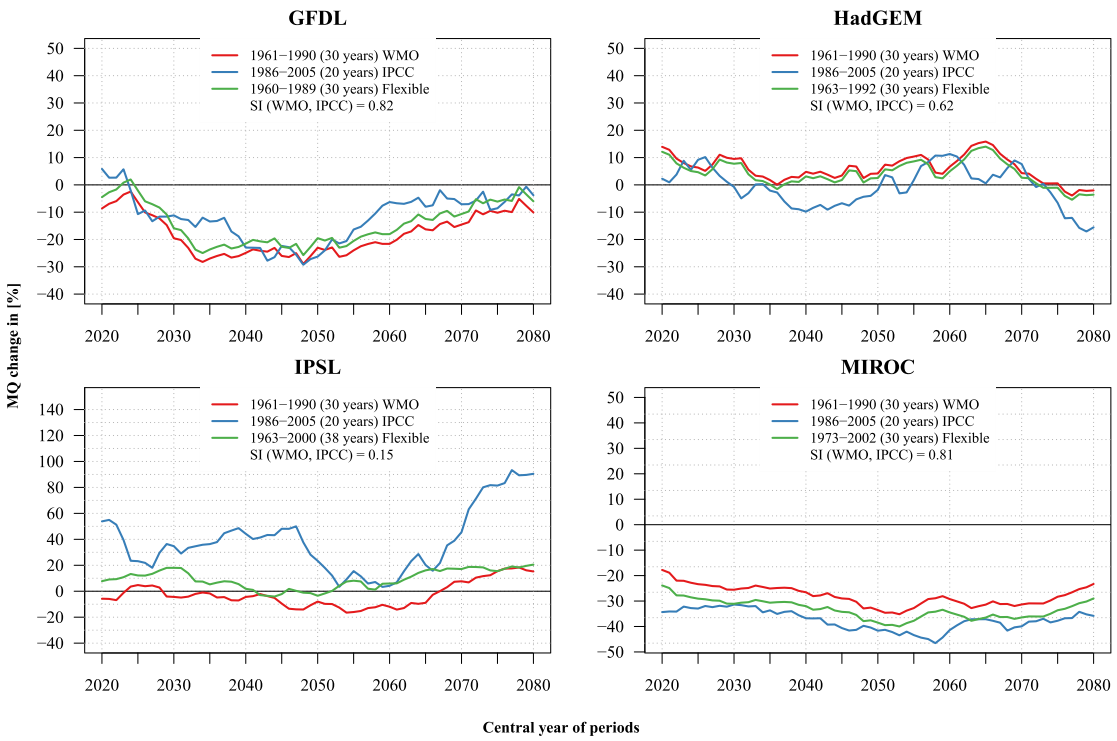

Figure C5. Relative change in mean discharge of central years. São Francisco River basin (SFC) under RCP 2.6. Changes are relative to mean annual discharge in WMO and IPCC baseline periods.

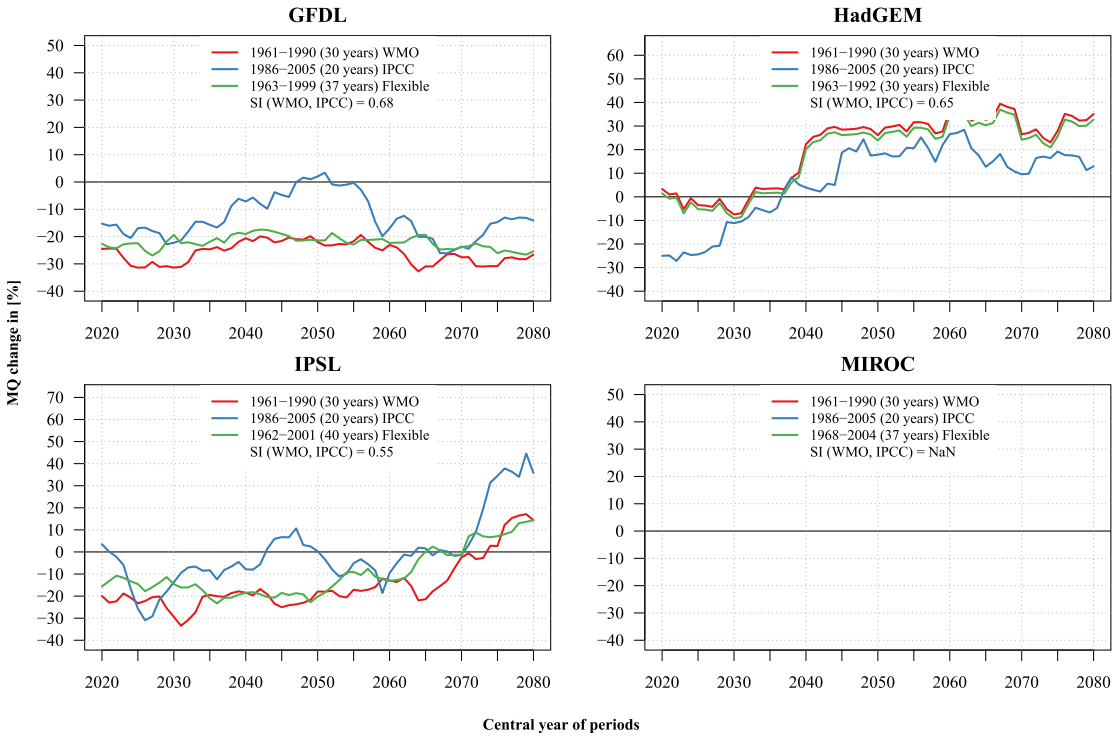

Figure C6. Relative change in mean discharge of central years. Tagus River basin (TAG) under RCP 2.6. Changes are relative to mean annual discharge in WMO and IPCC baseline periods.

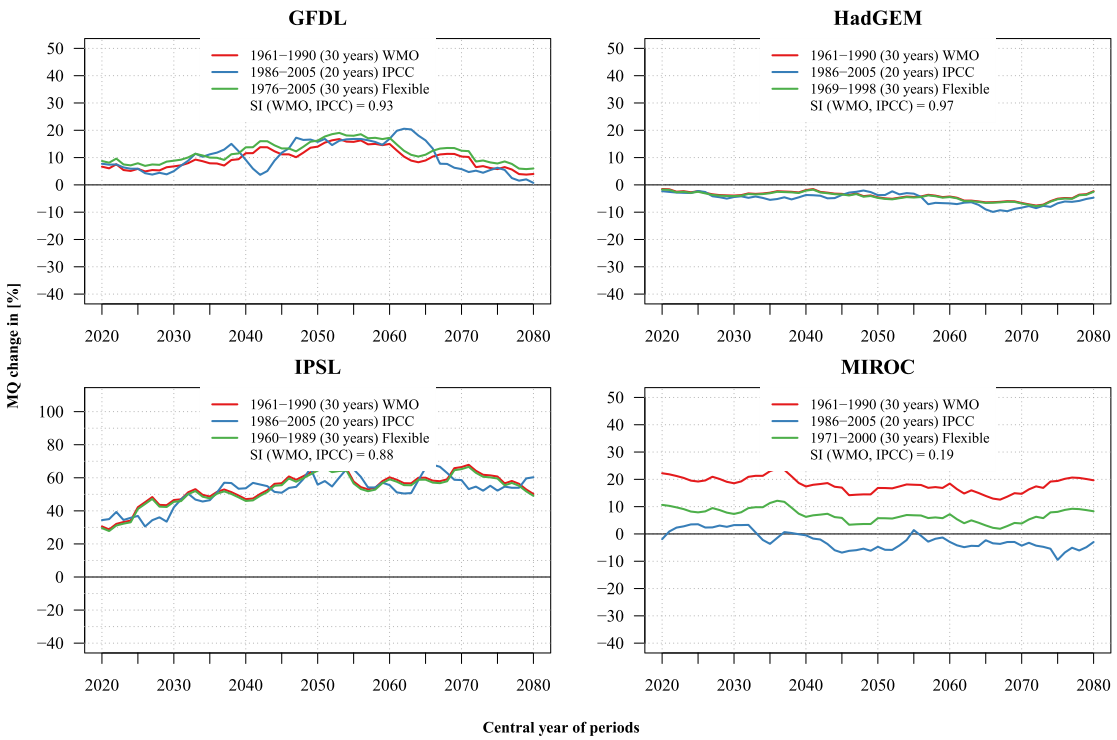

Figure C7. Relative change in mean discharge of central years. Upper Blue Nile River basin (UBN) under RCP 2.6. Changes are relative to mean annual discharge in WMO and IPCC baseline periods.

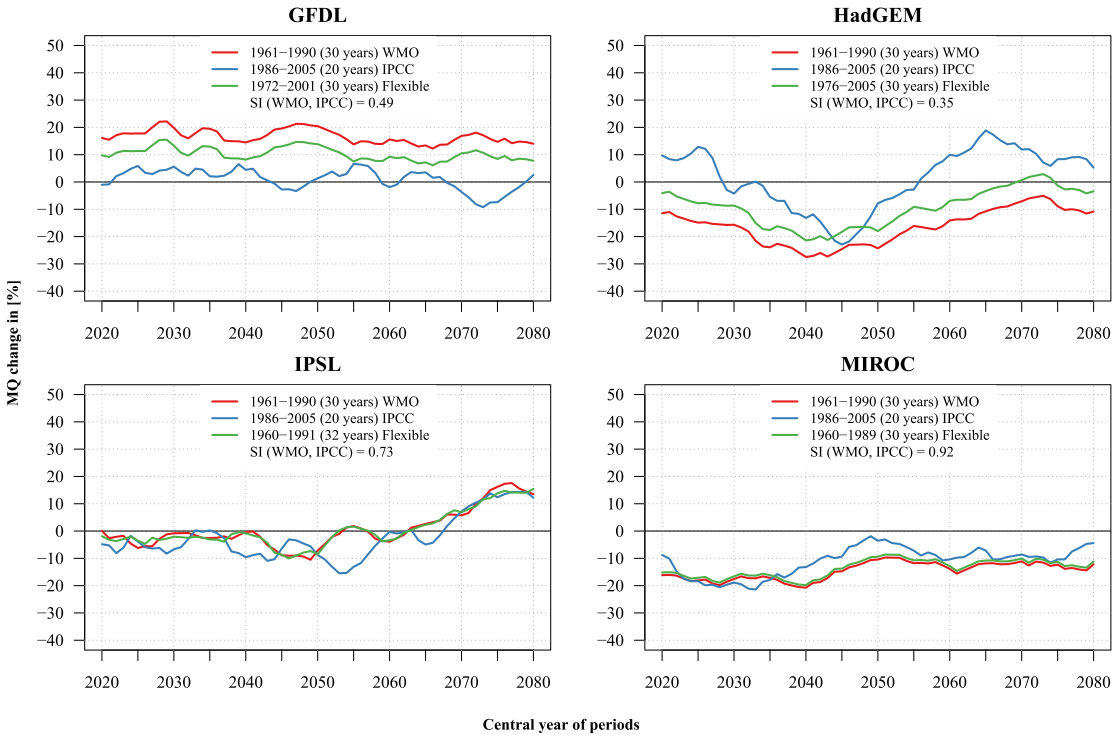

Figure C8. Relative change in mean discharge of central years. Upper Mississippi River basin (UMI) under RCP 2.6. Changes are relative to mean annual discharge in WMO and IPCC baseline periods.

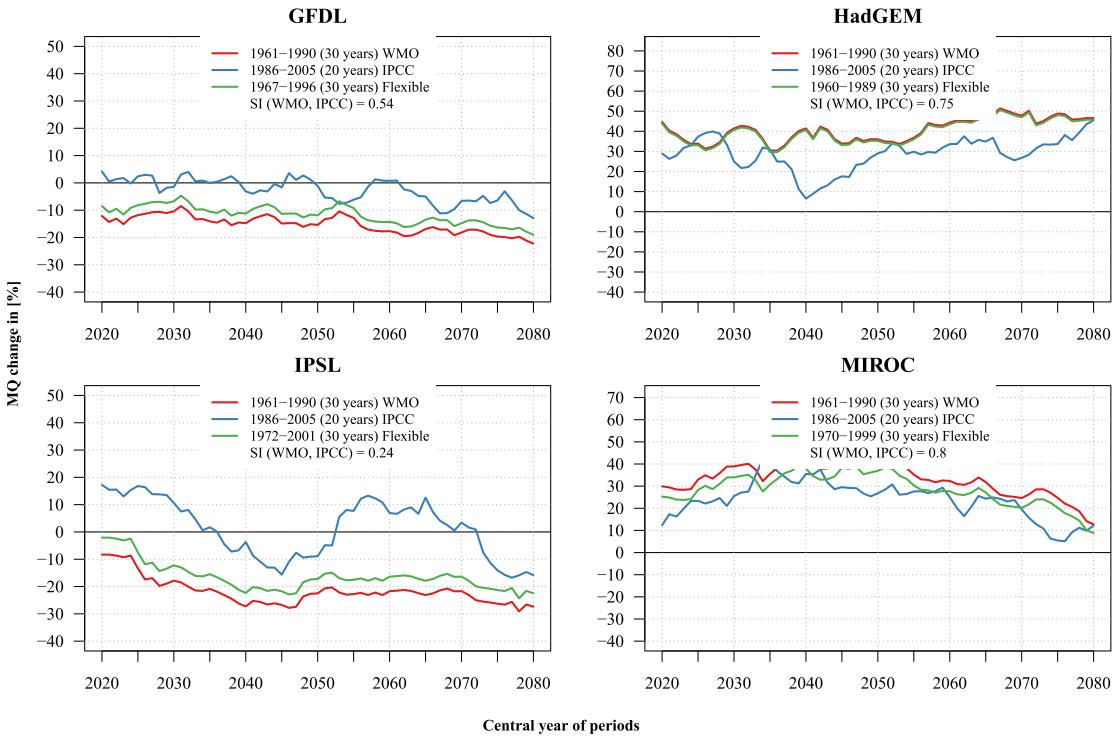

Figure C9. Relative change in mean discharge of central years. Volta River basin (VOL) under RCP 2.6. Changes are relative to mean annual discharge in WMO and IPCC baseline periods.

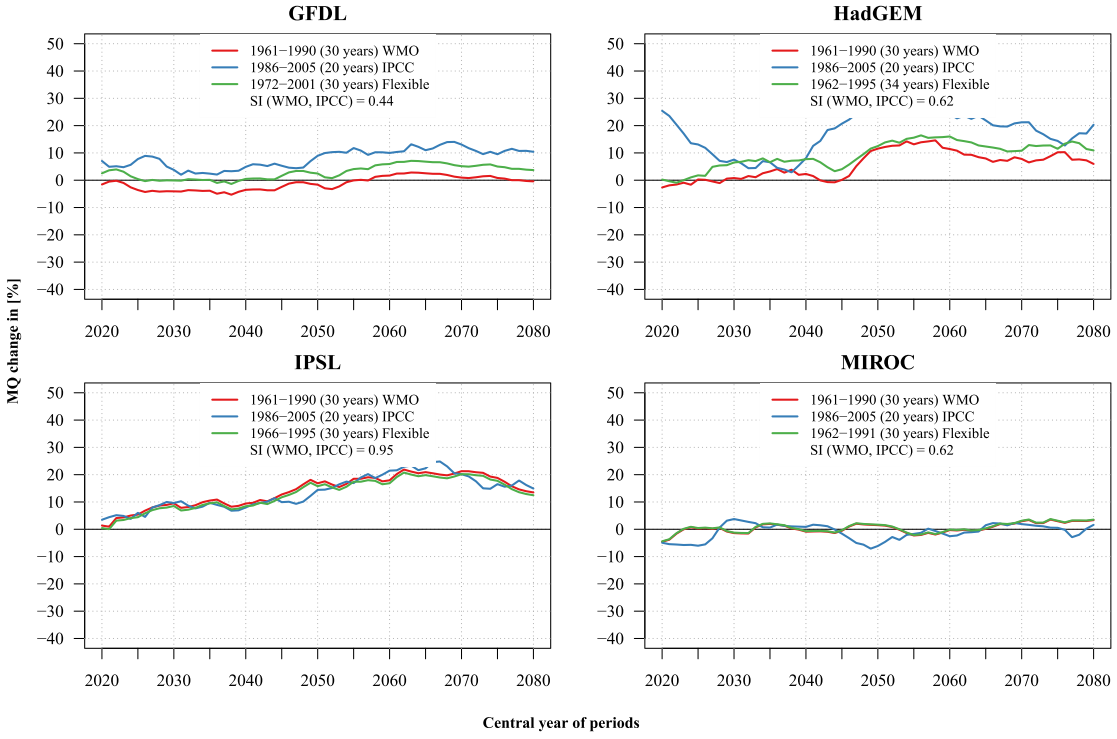

Figure C10. Relative change in mean discharge of central years. Upper Yellow River basin (YEL) under RCP 2.6. Changes are relative to mean annual discharge in WMO and IPCC baseline periods.

C.2. RCP 8.5

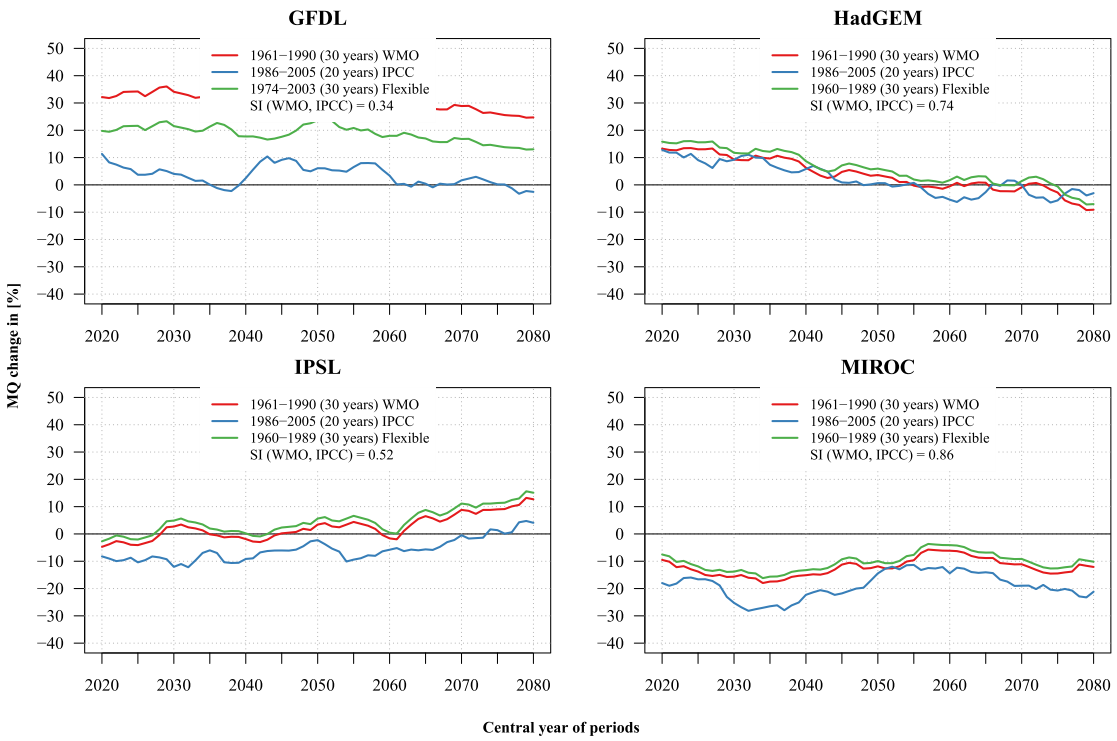

Figure C11. Relative change in mean discharge of central years. Northern Dvina River basin (DVI) under RCP 8.5. Changes are relative to mean annual discharge in WMO and IPCC baseline periods.

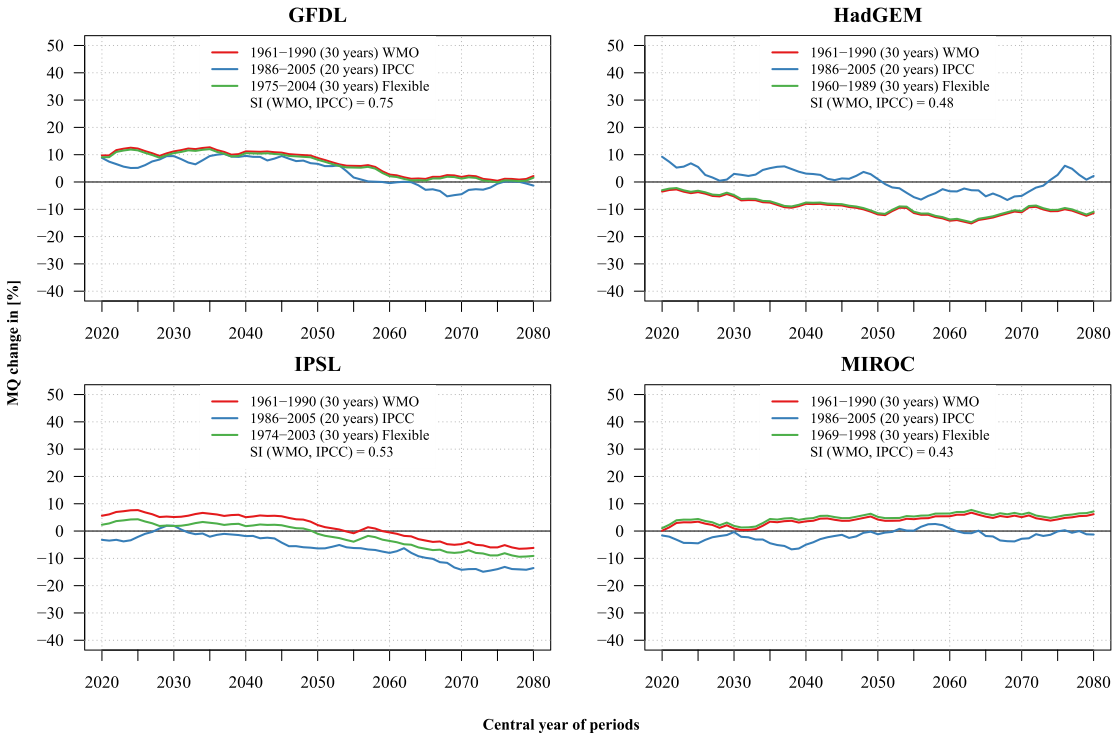

Figure C12. Relative change in mean discharge of central years. Rhine River basin (RHI) under RCP 8.5. Changes are relative to mean annual discharge in WMO and IPCC baseline periods.

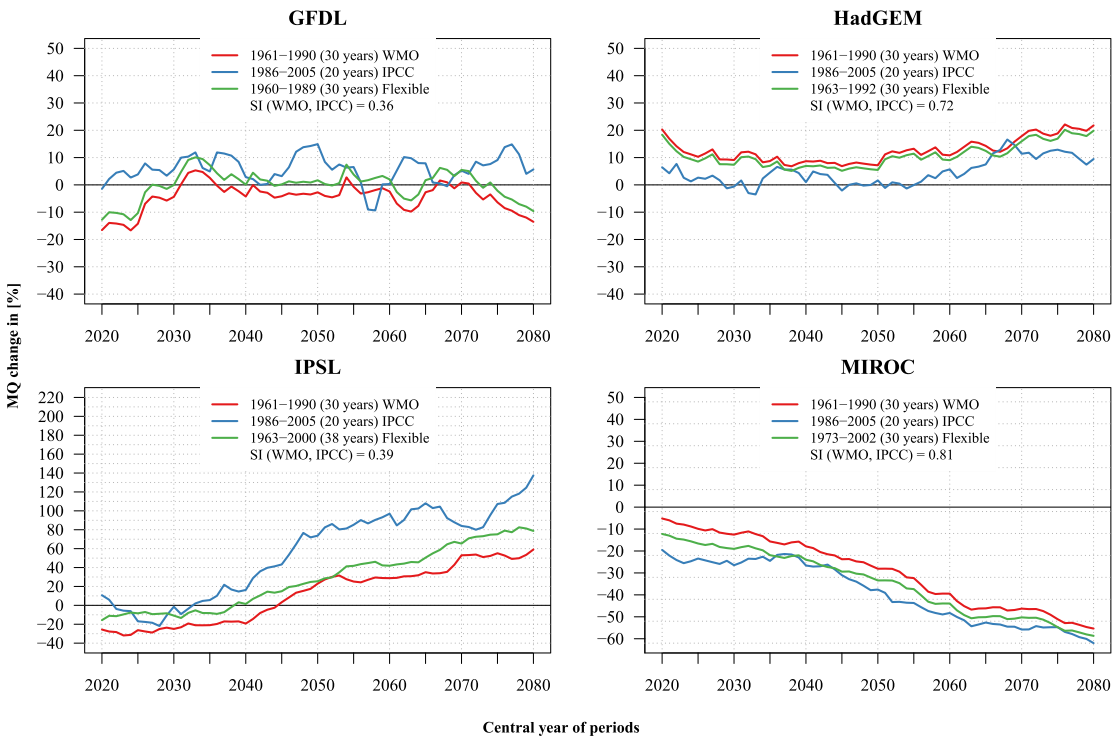

Figure C13. Relative change in mean discharge of central years. São Francisco River basin (SFC) under RCP 8.5. Changes are relative to mean annual discharge in WMO and IPCC baseline periods.

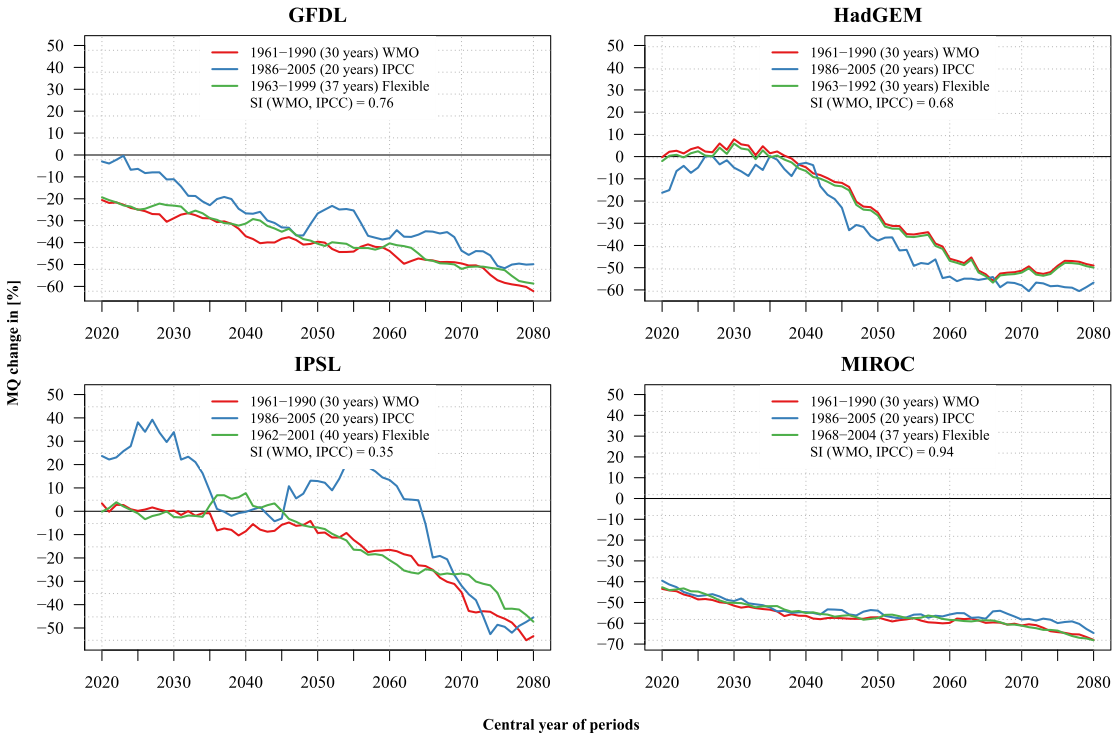

Figure C14. Relative change in mean discharge of central years. Tagus River basin (TAG) under RCP 8.5. Changes are relative to mean annual discharge in WMO and IPCC baseline periods.

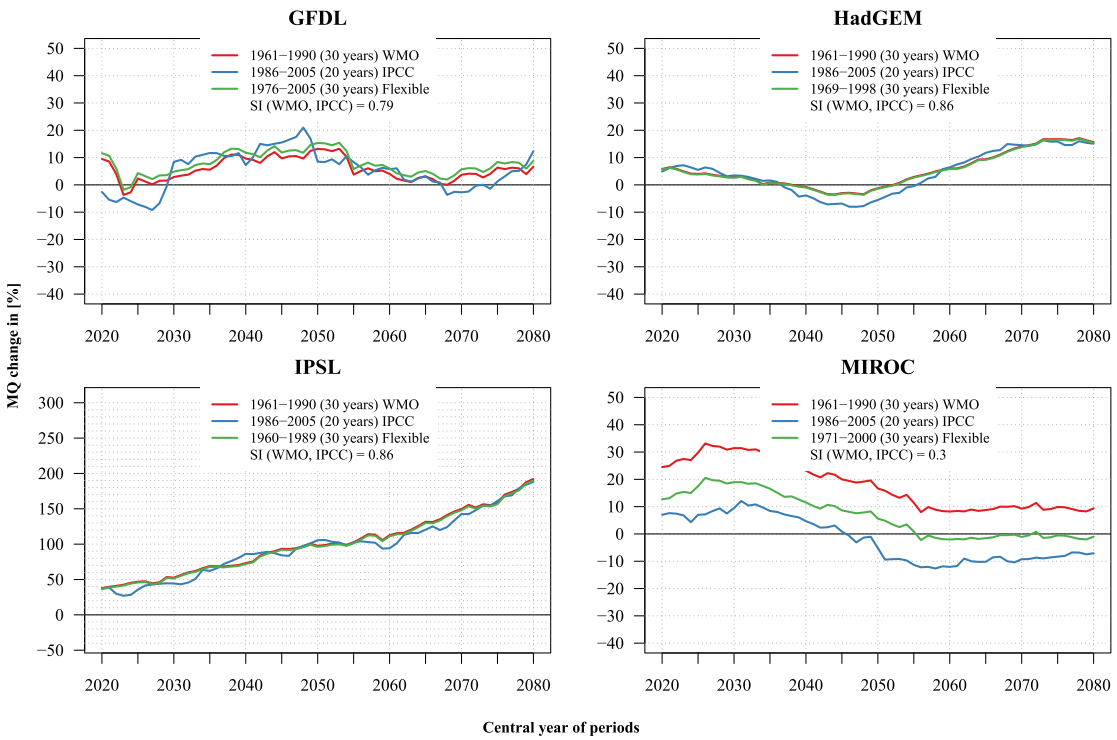

Figure C15. Relative change in mean discharge of central years. Upper Blue Nile River basin (UBN) under RCP 8.5. Changes are relative to mean annual discharge in WMO and IPCC baseline periods.

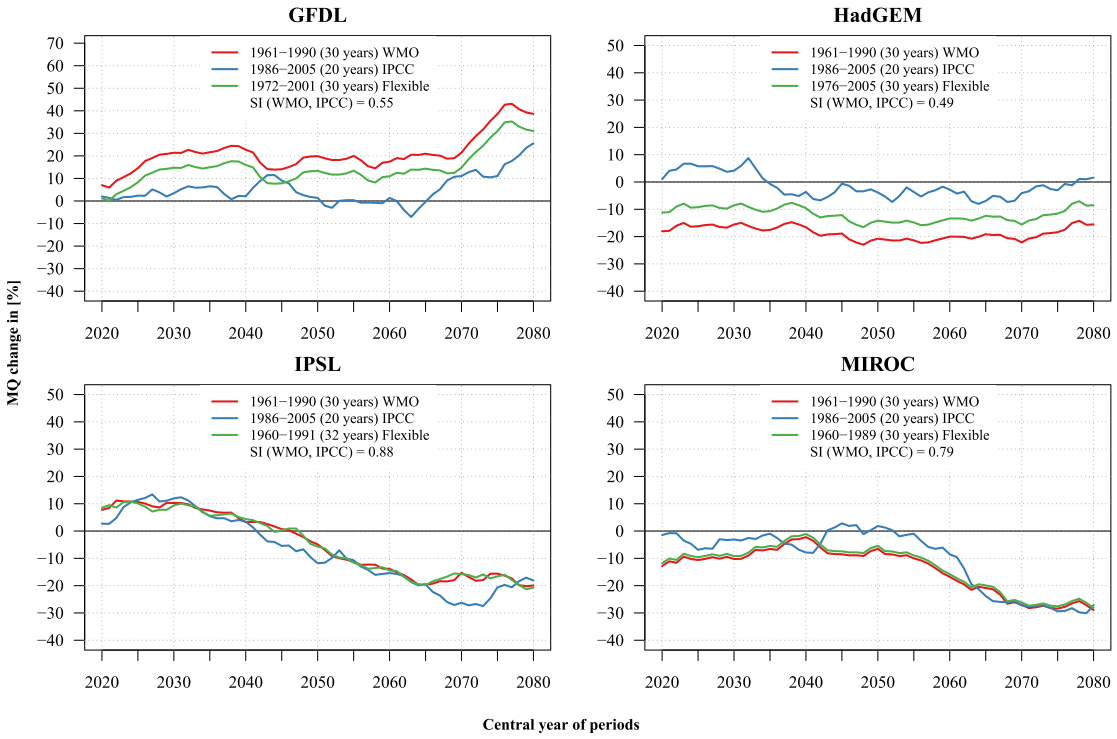

Figure C16. Relative change in mean discharge of central years. Upper Mississippi River basin (UMI) under RCP 8.5. Changes are relative to mean annual discharge in WMO and IPCC baseline periods.

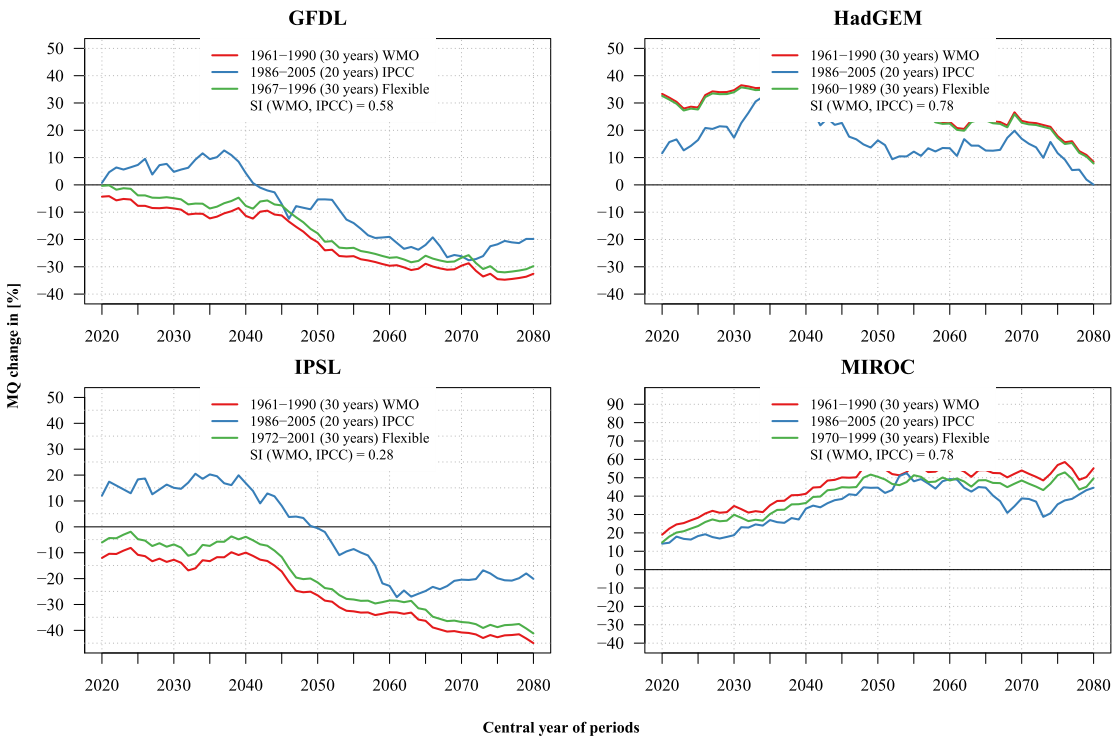

Figure C17. Relative change in mean discharge of central years. Volta River basin (VOL) under RCP 8.5. Changes are relative to mean annual discharge in WMO and IPCC baseline periods.

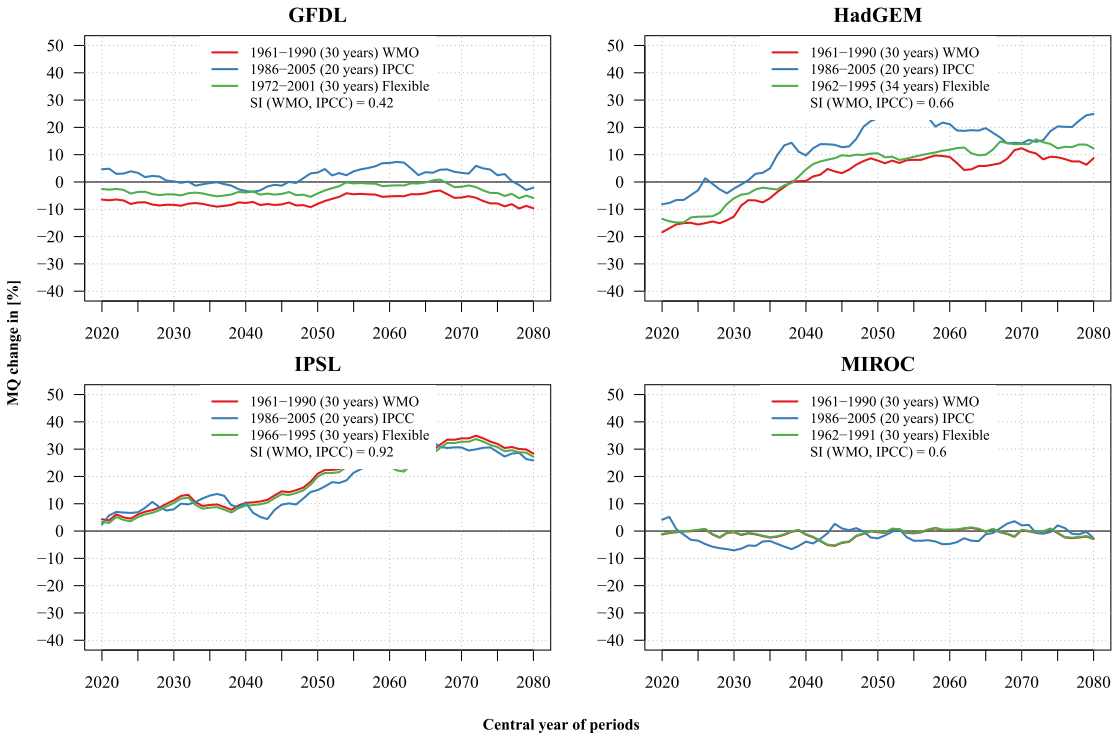

Figure C18. Relative change in mean discharge of central years. Upper Yellow River basin (YEL) under RCP 8.5. Changes are relative to mean annual discharge in WMO and IPCC baseline periods.

Appendix D. Similarity index

Table D1. Similarity index *SI* between WMO and IPCC ΔMQ series, RCP 8.5.

	DVI	RHI	SFC	TAG	UBN	UMI	VOL	YEL	Average
GFDL	0.34	0.75	0.36	0.76	0.79	0.55	0.58	0.42	0.57
HadGEM	0.74	0.48	0.72	0.68	0.86	0.49	0.78	0.66	0.68
IPSL	0.52	0.53	0.39	0.35	0.86	0.88	0.28	0.92	0.59
MIROC5	0.86	0.43	0.81	0.94	0.30	0.79	0.78	0.60	0.69
Average	0.62	0.55	0.57	0.68	0.70	0.68	0.61	0.65	

Appendix E. Ensemble mean

Table E2. Ensemble mean ΔMQ in selected future periods in [%] relative to *MQ* of WMO, IPCC, and flexible baseline, RCP 8.5.

	2040			2060			2080		
Basins	WMO	IPCC	Flex.	WMO	IPCC	Flex.	WMO	IPCC	Flex.
DVI	4.8	−5.8	3.3	5.5	−5.6	4.0	4.1	−5.7	2.7
RHI	3.0	1.5	2.3	−1.6	−2.7	−2.2	−2.3	−3.5	−2.8
SFC	−8.2	−1.6	−3.9	−0.6	13.7	2.3	3.0	22.6	7.6
TAG	−26.7	−21.1	−21.8	−41.5	−33.6	−41.8	−58.2	−54.2	−55.8
UBN	26.3	23.6	23.6	32.7	23.6	30.2	56.0	52.2	53.3
UMI	1.8	−1.5	2.4	−8.3	−6.3	−8.2	−6.5	−4.5	−6.6
VOL	14.6	20.4	15.6	3.6	5.2	3.9	−3.5	1.2	−3.4
YEL	0.4	3.2	2.2	7.3	13.4	8.7	6.1	11.5	7.7
Mean diff.	4.9			6.7			6.3		
Min. diff.	1.5			1.1			1.2		
Max. diff.	10.6			14.3			19.6		
Median diff.	4.5			7.0			4.4		

Last four rows indicate differences between WMO and IPCC ΔMQ series
Flex. = flexible baseline periods

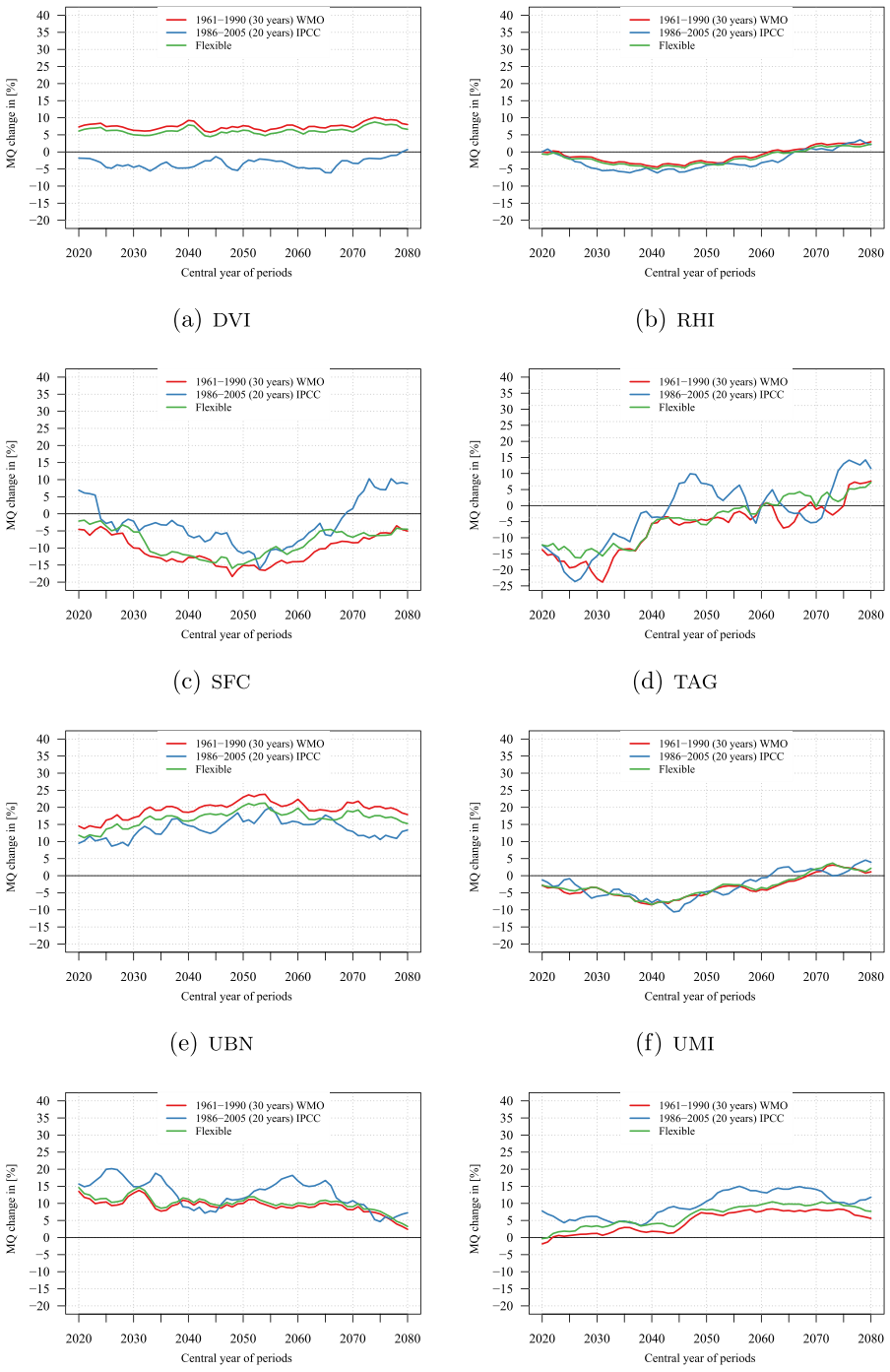

Figure E19. Relative change in mean discharge of central years using the ensemble mean under RCP 2.6. Changes are relative to mean annual discharge in WMO and IPCC baseline periods.

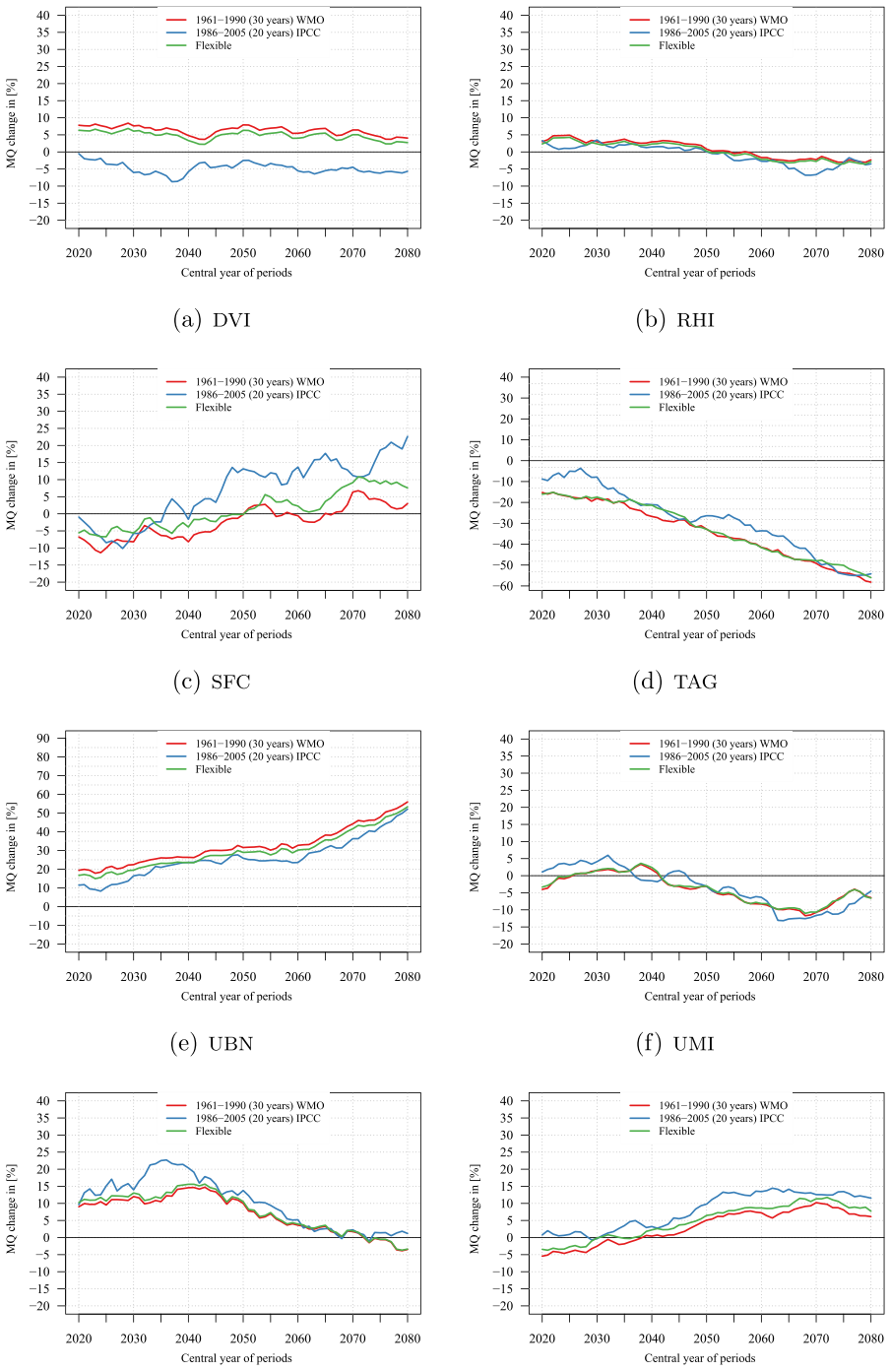

Figure E20. Relative change in mean discharge of central years using the ensemble mean under RCP 8.5. Changes are relative to mean annual discharge in WMO and IPCC baseline periods.

ORCID iDs

S Liersch https://orcid.org/0000-0003-2778-3861
T Pilz https://orcid.org/0000-0002-5641-3918
S Huang https://orcid.org/0000-0001-7426-5181
F F Hattermann https://orcid.org/0000-0002-6046-4670

References

[1] Porter J J and Dessai S 2017 Mini-me: Why do climate scientists' misunderstand users and their needs? *Environ Sci Policy* **77** 9–14
[2] Eyring V *et al* 2019 Taking climate model evaluation to the next level *Nat. Clim. Change* **9** 102–10
[3] Lorenz R, Herger N, Sedláček J, Eyring V, Fischer E M and Knutti R 2018 Prospects and Caveats of Weighting Climate Models for Summer Maximum Temperature Projections Over North America *J. Geophys. Res. Atmos.* **123** 4509–26
[4] Liersch S, Tecklenburg J, Rust H, Dobler A, Fischer M, Kruschke T, Koch H and Hattermann F F 2018 Are we using the right fuel to drive hydrological models? A climate impact study in the Upper Blue Nile *Hydrol. Earth Syst. Sci* **22** 2163–85
[5] Rowell P D, Senior A C, Vellinga M and Graham J R 2016 Can climate projection uncertainty be constrained over Africa using metrics of contemporary performance? *Clim. Change* **134** 621–33
[6] Latif M 2011 Can climate projection uncertainty be constrained over Africa using metrics of contemporary performance? Sustainability of Geochemical Cycling *J. Geochem. Explor.* **110** 1–7
[7] Bronstert A, Kolokotronis V, Schwandt D and Helmut S 2007 Comparison and evaluation of regional climate scenarios for hydrological impact analysis: General scheme and application example *Int. J. Climatol.* **27** 1579–94
[8] Krysanova V, Donnelly C, Gelfan A, Gerten D, Arheimer B, Hattermann F and Kundzewicz Z W 2018 How the performance of hydrological models relates to credibility of projections under climate change *Hydrolog Sci J* **63** 696–720
[9] Hattermann F F *et al* 2018 Sources of uncertainty in hydrological climate impact assessment: a cross-scale study *Environ. Res. Lett.* **13** 015006
[10] Vetter T *et al* 2017 Evaluation of sources of uncertainty in projected hydrological changes under climate change in 12 large-scale river basins *Clim. Change* **141** 419–33
[11] Kent C, Chadwick R and Rowell D P 2015 Understanding Uncertainties in Future Projections of Seasonal Tropical Precipitation *J. Clim.* **28** 4390–4413
[12] Remesan R and Holman I P 2015 Effect of baseline meteorological data selection on hydrological modelling of climate change scenarios *J. Hydrol.* **528** 631–42
[13] Elshamy M, di Baldassarre G and van Griensven A 2013 Characterizing Climate Model Uncertainty Using an Informal Bayesian Framework: Application to the River Nile *J Hydrol Eng. ASCE* **18** 582–9
[14] Knutti R and Sedlacek J 2013 Robustness and uncertainties in the new CMIP5 climate model projections *Nature Clim. Change* **3** advance online publication 369–373
[15] Teutschbein C and Seibert J 2012 Bias correction of regional climate model simulations for hydrological climate-change impact studies: Review and evaluation of different methods *J. Hydrol.* **456-457** 12–29
[16] WMO 2007 The role of climatological normals in a changing climate Tech. Rep. WMO/TD-No. 1377; WCDMP-No. 61 World Meteorological Organization (WMO) (https://library.wmo.int/doc_num.php?explnum_id=4546)
[17] WMO 2014 (https://public.wmo.int/en/media/press-release/no-997-scientists-urge-more-frequent-updates-of-30-year-climate-baselines-keep)
[18] Hawkins E and Sutton R 2016 Connecting Climate Model Projections of Global Temperature Change with the Real World *Bull. Am. Meteorol. Soc.* **97** 963–80
[19] WMO 2017 WMO Guidelines on the Calculation of Climate Normals Tech. Rep. WMO- No. 1203 World Meteorological Organization (WMO) (https://library.wmo.int/doc_num.php?explnum_id=4166)
[20] IPCC 2014 Climate Change 2014: Synthesis Report. Contribution of Working Groups I, II and III to the Fifth Assessment Report of the Intergovernmental Panel on Climate Change Tech. rep. Intergovernmental Panel on Climate Change (https://www.ipcc.ch/report/ar5/syr/)
[21] Kravtsov S, Grimm C and Gu S 2018 Global-scale multidecadal variability missing in state-of-the-art climate models *npj Climate and Atmospheric Science* **1** 34
[22] Ruokolainen L and Räisänen J 2007 Probabilistic forecasts of near-term climate change: sensitivity to adjustment of simulated variability and choice of baseline period *Tellus A: Dynamic Meteorology and Oceanography* **59** 309–20
[23] Razavi S, Elshorbagy A, Wheater H and Sauchyn D 2015 Toward understanding nonstationarity in climate and hydrology through tree ring proxy records *Water Resour. Res.* **51** 1813–30
[24] Huang S, Kumar R, Rakovec O, Aich V, Wang X, Samaniego L,, Liersch S and Krysanova V 2018 Multimodel assessment of flood characteristics in four large river basins at global warming of 1.5, 2.0 and 3.0 K above the pre-industrial level *Environ. Res. Lett.* **13** 124005
[25] Snell R S, Elkin C, Kotlarski S and Bugmann H 2018 Importance of climate uncertainty for projections of forest ecosystem services *Regional Environmental Change* **18** 2145–59
[26] Baker D J, Hartley A J, Butchart S H M and Willis S G 2016 Choice of baseline climate data impacts projected species' responses to climate change *Global Change Biology* **22** 2392–404
[27] Warszawski L, Frieler K, Huber V, Piontek F, Serdeczny O and Schewe J 2014 *PNAS* vol 111 pp 3228–32 The Inter-Sectoral Impact Model Intercomparison Project (ISI–MIP): Project framework (https://doi.org/10.1073/pnas.1312330110)
[28] Huber V *et al* 2014 Climate impact research: beyond patchwork *Earth System Dynamics* **5** 399–408
[29] Hempel S, Frieler K, Warszawski L, Schewe J and Piontek F 2013 A trend-preserving bias correction – the ISI-MIP approach *Earth System Dynamics Discussions* **4** 49–92
[30] Kottek M, Grieser J, Beck C, Rudolf B and Rubel F 2006 World Map of the Köppen-Geiger climate classification updated *Meteorol. Z.* **15** 259–63
[31] Lobanova A, Liersch S and Nunes J P *et al* 2018 Hydrological impacts of moderate and high-end climate change across European river basins *J. Hydrol. Reg. Stud.* **18** 15–30
[32] Koch H, Liersch S, Azevedo J R G D, Silva A L C and Hattermann F F 2018 Assessment of observed and simulated low flow indices for a highly managed river basin *Hydrology Research* **49** 1831–46
[33] Liersch S, Koch H and Hattermann F F 2017 Management Scenarios of the Grand Ethiopian Renaissance Dam and Their Impacts under Recent and Future Climates *Water* **9** 728
[34] Aich V *et al* 2014 Comparing impacts of climate change on streamflow in four large African river basins *Hydrol. Earth Syst. Sci* **18** 1305–21
[35] Krysanova V, Müller-Wohlfeil D I and Becker A 1998 Development and test of a spatially distributed hydrological/water quality model for mesoscale watersheds *Ecological Modelling* **106** 261–89
[36] Krysanova V, Hattermann F and Wechsung F 2005 Development of the ecohydrological model SWIM for regional impact studies and vulnerability assessment *Hydrol. Process.* **19** 763–83
[37] Frieler K *et al* 2017 Assessing the impacts of 1.5°C global warming – simulation protocol of the Inter-Sectoral Impact

Model Intercomparison Project (ISIMIP2b) *Geoscientific Model Development* **10** 4321–45

[38] Trenberth K E, Dai A, van der Schrier G, Jones P D, Barichivich J, Briffa K R and Sheffield J 2014 Global warming and changes in drought *Nat. Clim. Change* **4** 17–22

[39] Wigley T M L and Raper S C B 2001 Interpretation of High Projections for Global-Mean Warming *Science* **293** 451–4